

Variations in Image-Based Radiomic Measures of the Rotator Cuff Muscles by Indication for Total Shoulder Arthroplasty

Josie Elwell¹, Gregory Spangenberg¹, Hamidreza Rajabzadeh-Oghaz¹, William R. Aibinder², Bradley Schoch³, Bruno Gobbato⁴, Scott W. Trenhaile⁵, Anshuman Singh⁶, John Erickson⁷, Christopher P. Roche¹

¹Advita Ortho, Gainesville, FL, USA, ²University of Michigan, Ann Arbor, MI, USA, ³Mayo Clinic, Jacksonville, FL, USA, ⁴R. José Emmendoerfer, Jaraguá do Sul, SC, Brazil, ⁵Orthollinois, Rockford, IL, USA, ⁶University of California, San Diego, San Diego, CA, ⁷Atlantic Medical Group, New Providence, NJ, USA

Disclosures: J. Elwell: 3A; Advita Ortho. H. Rajabzadeh-Oghaz: 3A; Advita Ortho. G. Spangenberg: 3A; Advita Ortho. W. Aibinder: 3B; Advita Ortho. B. Schoch: 3B; Advita Ortho. B. Gobbato: 3B; Advita Ortho. S. Trenhaile: 3B; Advita Ortho. A. Singh: 3B; Advita Ortho. J. Erickson: 3B; Advita Ortho. C. Roche: 3A; Advita Ortho.

INTRODUCTION: The condition of the rotator cuff muscles is a key consideration in treatment decision-making for total shoulder arthroplasty (TSA), as it impacts the decision between implant types, namely anatomic TSA (aTSA) versus reverse TSA (rTSA), as well as the potential outcomes of the procedure. Currently, the rotator cuff muscles are subjectively assessed via medical imaging on crude quantitative scales (e.g. tear size and relative amount of fatty infiltration). However, rotator cuff tears and associated pathological changes to the muscles likely exist on a broad spectrum that is not sufficiently captured by these assessments. Objective, automatic quantification of medical images at a large scale offers the potential to investigate differences in shape and intensity-based radiomic measures of the muscles between patients with and without rotator cuff pathologies, which was the objective of this study.

METHODS: Patients undergoing primary total shoulder arthroplasty with a single, platform system and available pre-operative CT scans were eligible for inclusion. Those with a diagnosis other than osteoarthritis (OA), rotator cuff tear (RCT), and/or cuff tear arthropathy (CTA) were excluded. An automated, machine-learning based segmentation algorithm identified the boundaries of each of the four rotator cuff muscles in the CT scans. CT scans were then pre-processed to normalize the Hounsfield Unit (HU) value of each voxel based on the Z-score. For each muscle, six radiomic measures were then quantified, including five shape (volume, surface-to-volume ratio [STV], elongation, flatness, and sphericity) and one intensity-based (mean HU) using PyRadiomics¹ (v3.0.1). Radiomic measures (examples shown in Figure 1) were then compared, between cohorts with and without rotator cuff pathology (RCP). The cohort without RCP included patients that had a diagnosis of OA only, whereas the cohort with RCP included any patient with a diagnosis of RCT (with or without OA) or CTA. Cohorts were compared using non-parametric Wilcoxon rank sum tests with significance set at $p < 0.05$ and analyses were performed including all patients and then stratified by males and females only.

RESULTS SECTION: In total, 4,935 patients were included in the study, of which 61.8% (3,049) were diagnosed with OA only and 38.2% (1,886) were diagnosed with RCP. The OA cohort was significantly younger (68.9 ± 8.7 vs 71.8 ± 7.6 , $p < 0.001$), had significantly less females (48.8% vs 51.7% $p = 0.043$), and had significantly higher BMI (30.2 ± 6.3 vs 29.2 ± 6.1 , $p < 0.001$). Out of 24 total radiomic measures (six for each muscle), there were significant differences in every measure between the OA and RCP cohorts, except for mean HU of the supraspinatus and teres minor, as well as elongation of teres minor (Table 1). When considering males only the OA cohort was also significantly younger (67.2 ± 8.8 vs 70.9 ± 7.9 , $p < 0.001$) and had significantly higher BMI (30.4 ± 5.4 vs 29.3 ± 5.1 , $p < 0.001$). Similar to the analysis including all patients, the only measures that were not significantly different between cohorts were mean HU of the supraspinatus/teres minor and elongation of teres minor (Table 1). Considering females only, the OA cohort was significantly younger (70.7 ± 8.2 vs 72.6 ± 7.2 , $p < 0.001$) and had significantly higher BMI (30.0 ± 7.0 vs 29.2 ± 6.9 , $p < 0.001$). There were comparatively more measures that were not significantly different between pathology cohorts (infraspinatus: 0, subscapularis: 2, supraspinatus: 3, teres minor: 3).

DISCUSSION: This study found significant differences in a large portion of the selected radiomic measures of the rotator cuff between cohorts with and without rotator cuff pathology. These differences were less prevalent considering female patients only compared to all patients and male patients only. Interestingly both the volume and sphericity of the muscles in OA patients was universally greater for the supraspinatus, subscapularis, and infraspinatus, but less for teres minor compared to RCP patients. Lower volume in RCP patients may be expected as a result of muscle mass loss with age, and it should be noted that these patients were significantly older. However, since the supraspinatus is the most commonly torn tendon, followed by the infraspinatus, subscapularis, and teres minor, greater volume of teres minor in RCP patients may be indicative of hypertrophy to compensate for external rotation weakness in the setting of supraspinatus and/or infraspinatus tears and associated atrophy. On the contrary, mean HU, which is theoretically correlated to muscle quality and the relative amount of fatty infiltration, was not significantly different between OA and RCP cohorts for the supraspinatus or teres minor, but was significantly lower in the OA cohort for the subscapularis and significantly higher in the infraspinatus. One limitation of this study is the retrospective, multi-center nature, which results in variability in reconstruction kernels of the CT scans and likely impacts the quantification of intensity-based metrics. This potentially explains the lack of findings related to mean HU. Other limitations of include the small number of radiomic measures studied, where there may be other measures that are more distinguished between pathologic cohorts. Finally, it is currently unknown how differences in these radiomic measures impact both pre- and post-operative function of shoulders implanted with TSA and future work should seek to investigate these relationships to potentially aid diagnosis, treatment decision-making and patient counseling.

SIGNIFICANCE/CLINICAL RELEVANCE: Significant differences in radiomic measures of the rotator cuff musculature between patients with and without rotator cuff pathologies were observed. These features are automatically quantified from pre-operative, standard of care medical images and could eventually aid in understanding pathological changes to the musculature that occur as a result of rotator cuff tears as they relate to both diagnosis and treatment decision-making for total shoulder arthroplasty.

REFERENCES: [1] van Griethuysen, J. J. M., et al. (2017). Computational Radiomics System to Decode the Radiographic Phenotype. *Cancer Research*, 77(21), e104–e107.

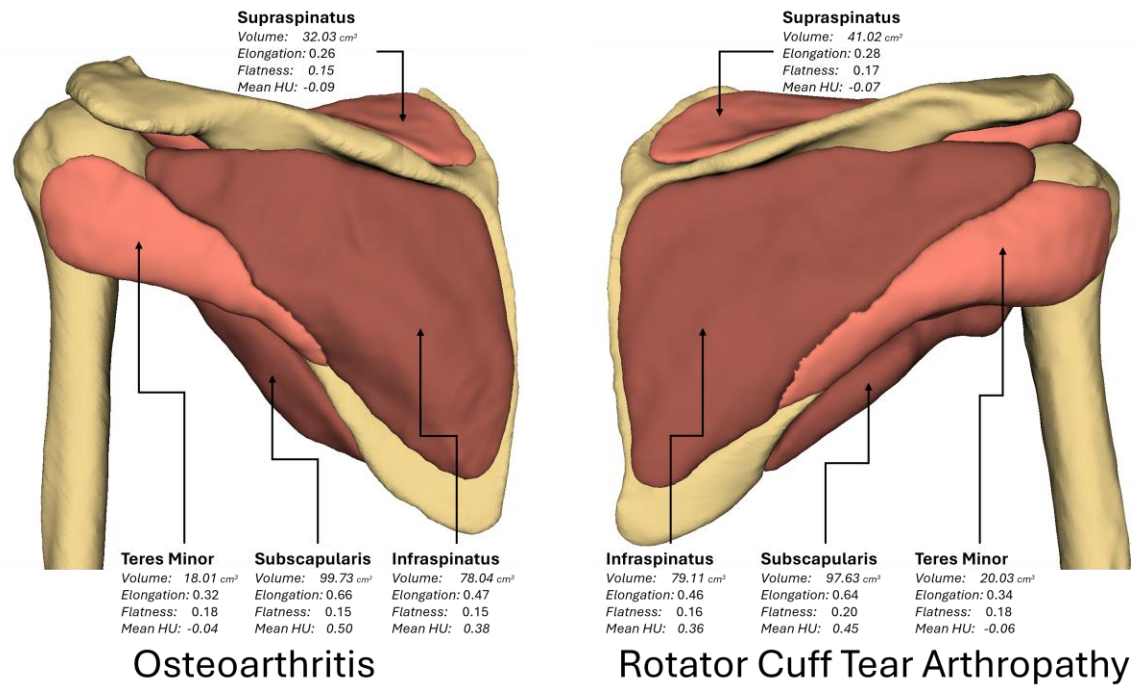


Figure 1. Radiomic measurements of the rotator cuff for a patient with Osteoarthritis (left) and with Cuff Tear Arthropathy (right).

Table 1. Differences in radiomic measures of the rotator cuff muscles in OA vs RTCP patients including all patients and stratified by male and female patients only.

Muscle	Measure	All Patients			Males Only			Females Only		
		OA	RTCP	p-value	OA	RTCP	p-value	OA	RTCP	p-value
Supra	Volume [cm ³]	51.11 ± 15.65	45.65 ± 13.38	<0.001	62.47 ± 12.62	55.8 ± 11.1	<0.001	39.18 ± 7.57	36.18 ± 6.74	<0.001
	STV	0.23 ± 0.03	0.25 ± 0.03	<0.001	0.22 ± 0.02	0.23 ± 0.02	<0.001	0.25 ± 0.02	0.26 ± 0.02	<0.001
	Elongation	0.30 ± 0.03	0.3 ± 0.04	<0.001	0.32 ± 0.03	0.31 ± 0.04	<0.001	0.29 ± 0.03	0.29 ± 0.04	0.518
	Flatness	0.19 ± 0.03	0.18 ± 0.03	<0.001	0.19 ± 0.03	0.18 ± 0.03	<0.001	0.18 ± 0.02	0.18 ± 0.03	0.285
	Sphericity	0.57 ± 0.03	0.56 ± 0.03	<0.001	0.57 ± 0.03	0.55 ± 0.03	<0.001	0.57 ± 0.03	0.57 ± 0.03	<0.001
	Mean HU	-0.08 ± 0.14	-0.08 ± 0.14	0.324	-0.1 ± 0.13	-0.09 ± 0.14	0.782	-0.06 ± 0.14	-0.07 ± 0.15	0.060
Subscap	Volume [cm ³]	147.69 ± 49	136.52 ± 43.01	<0.001	183.86 ± 38.38	168.91 ± 36.18	<0.001	109.68 ± 23.57	106.33 ± 21.56	0.001
	STV	0.20 ± 0.03	0.21 ± 0.03	<0.001	0.18 ± 0.03	0.19 ± 0.03	<0.001	0.22 ± 0.03	0.22 ± 0.03	0.138
	Elongation	0.72 ± 0.08	0.68 ± 0.07	<0.001	0.75 ± 0.07	0.71 ± 0.08	<0.001	0.69 ± 0.07	0.66 ± 0.07	<0.001
	Flatness	0.21 ± 0.03	0.19 ± 0.03	<0.001	0.21 ± 0.03	0.2 ± 0.03	<0.001	0.20 ± 0.03	0.19 ± 0.03	<0.001
	Sphericity	0.48 ± 0.04	0.47 ± 0.04	0.002	0.48 ± 0.04	0.47 ± 0.04	<0.001	0.47 ± 0.03	0.47 ± 0.03	0.727
	Mean HU	0.36 ± 0.10	0.39 ± 0.10	<0.001	0.34 ± 0.09	0.38 ± 0.1	<0.001	0.38 ± 0.10	0.39 ± 0.11	<0.001
Infra	Volume [cm ³]	109.8 ± 38.6	92.12 ± 30.02	<0.001	138.09 ± 31.1	113.58 ± 27.12	<0.001	80.08 ± 17.75	72.08 ± 14.99	<0.001
	STV	0.19 ± 0.04	0.22 ± 0.04	<0.001	0.17 ± 0.02	0.20 ± 0.05	<0.001	0.21 ± 0.03	0.23 ± 0.03	<0.001
	Elongation	0.50 ± 0.04	0.49 ± 0.04	<0.001	0.50 ± 0.04	0.49 ± 0.05	<0.001	0.49 ± 0.04	0.49 ± 0.04	0.003
	Flatness	0.18 ± 0.03	0.16 ± 0.03	<0.001	0.19 ± 0.03	0.16 ± 0.03	<0.001	0.17 ± 0.03	0.16 ± 0.03	<0.001
	Sphericity	0.55 ± 0.04	0.52 ± 0.04	<0.001	0.56 ± 0.04	0.52 ± 0.04	<0.001	0.53 ± 0.04	0.51 ± 0.04	<0.001
	Mean HU	0.36 ± 0.13	0.33 ± 0.14	<0.001	0.34 ± 0.13	0.31 ± 0.14	<0.001	0.38 ± 0.13	0.34 ± 0.14	<0.001
Teres Minor	Volume [cm ³]	25.02 ± 9.13	26.08 ± 9.68	<0.001	29.95 ± 8.93	31.37 ± 10.08	<0.001	19.84 ± 5.91	21.16 ± 6.02	<0.001
	STV	0.33 ± 0.05	0.31 ± 0.06	<0.001	0.32 ± 0.05	0.30 ± 0.06	<0.001	0.35 ± 0.05	0.33 ± 0.05	<0.001
	Elongation	0.28 ± 0.04	0.28 ± 0.05	0.626	0.28 ± 0.04	0.28 ± 0.05	0.130	0.28 ± 0.04	0.28 ± 0.05	0.350
	Flatness	0.17 ± 0.03	0.16 ± 0.03	<0.001	0.17 ± 0.03	0.16 ± 0.03	<0.001	0.16 ± 0.03	0.16 ± 0.03	0.140
	Sphericity	0.52 ± 0.04	0.54 ± 0.04	<0.001	0.51 ± 0.04	0.54 ± 0.04	<0.001	0.53 ± 0.03	0.55 ± 0.04	<0.001
	Mean HU	-0.02 ± 0.13	-0.02 ± 0.14	0.885	-0.04 ± 0.13	-0.05 ± 0.14	0.871	0.01 ± 0.13	0.00 ± 0.13	0.983